Available online at www.sciencedirect.com
SCIENCE DIRECT®
Journal of Solid State Chemistry 177 (2004) 3843–3848
JOURNAL OF SOLID STATE CHEMISTRY
http://elsevier.com/locate/jssc

Rapid Communication

Microwave hydrothermal flash synthesis of nanocomposites Fe–Co alloy/cobalt ferrite

T. Caillot,[a,*] G. Pourroy,[b] and D. Stuerga[c]

[a] *Laboratoire d'Application de la Chimie à l'Environnement (LACE), Université Claude Bernard Lyon 1, UMR CNRS 5634, 43 Boulevard du 11 Novembre 1918, 69622 Villeurbanne Cedex, France*

[b] *GERM (Groupe d'Etudes et de Recherches sur les Microondes), Laboratoire de Recherche sur la Réactivité des Solides, UMR 5613 CNRS-Université de bourgogne, BP 47870, 21078 Dijon Cedex, France*

[c] *Institut de Physique et de Chimie des Matériaux de Strasbourg, 23, rue du Lœss, BP 43, 67034 Strasbourg Cedex 2, France*

Received 21 April 2004; received in revised form 2 June 2004; accepted 6 June 2004

Available online 27 August 2004

Abstract

The present article presents, for the first time, the last developments reported for an original microwave hydrothermal flash synthesis of Fe–Co alloys (Fe_yCo_{1-y})/cobalt ferrite ($Fe_{3-x}Co_xO_4$) nanocomposites. Synthesis was performed in alcoholic solutions of ferrous chloride, cobalt chloride and sodium ethoxide (EtONa) using a microwave autoclave (The RAMO system) specially designed by authors. Compared with conventional synthesis, smaller grains (100 nm compared to 1 μm) can be produced in a short period (e.g. 10 s) using a less basic medium. In all the cases, the microstructure and the amount of metal inside the composite particles are very different from the product obtained via a classical route. Indeed, 20% of metal was routinely obtained using the microwave flash synthesis. Nevertheless, this mean of production is more efficient and much faster than the ones commonly used to produce this type of nanocomposites.

Keywords: Microwave; Hydrothermal; Synthesis; Nanocomposites; Fe–Co alloys; Cobalt ferrite

1. Introduction

Composite materials have given rise to numerous studies since the combination of different materials can drastically improve the overall properties achieved when only one of them is involved [1].

Fe–Co alloy/cobalt ferrite composites can be used for their interesting catalytic behavior during the hydrogenation of carbon monoxide. Indeed, they favor the formation of olefins without producing high amounts of CO_2 [2]. Their main interest is to reduce necessary treatment for them to be active in the Fischer–Tropsch process. However, the catalyst, and particularly the spinel phase, must be protected against both reduction and subsequent carburization; one of the solutions consists on exposing the catalyst to inert atmosphere during heating from ambient to work temperature (200°C) [3]. Fe–Co alloy/cobalt ferrite composites are also synthesized for their magnetic properties. Couplings between both phases have been observed [4,5]. Coercive fields and remanent magnetizations depend on composition and grain size. Small grain sized composites present high coercive field but lower remanent magnetization.

The production of nanocomposites with targeted chemical, mechanical or magnetic properties requires a great deal of expertise and a total control of each stage during the synthesis. Various methods have been explored, such as reduction of oxide in silica or alumina or high-energy ball-milling [6–12]. The synthesis of metal/spinel composite is generally based on the disproportionation of iron hydroxide into metallic iron and magnetite. This reaction takes place in aqueous solution using the precipitation of hydroxide in boiling KOH [13,14]. When Co(II) is involved, the oxide part consists on a cobalt-substituted magnetite and the metallic part is an iron–cobalt alloy due to the partial

*Corresponding author. Fax: +33-4-72-44-81-14.
E-mail address: thierry.caillot@univ-lyon1.fr (T. Caillot).

0022-4596/$ - see front matter © 2004 Elsevier Inc. All rights reserved.
doi:10.1016/j.jssc.2004.06.009

reduction of Co(II) by metallic iron [15,16]. The disproportionation can also be obtained in an alcoholic medium (where EtONa acts as a base) using a microwave heating source [17]. In this case, solutions of ferrous chloride in sodium ethoxide lead in a very short time (few seconds to minutes) to a range of iron compounds as hematite, magnetite or iron-magnetite nanocomposites. For example, the microwave heating based technique allows the production of nanocomposites build around metallic iron and magnetite phase only when $[EtO^-] > 2\,[Fe^{2+}]$ and $[EtO^-] > 0.4$ M. Those "microwave produced" composites are 10–20 nm in size and their synthesis needs a less basic medium (1 M EtONa). This is important to note at this point that similar composites produced in boiling KOH with conventional heating have much larger grains (100–2000 nm) and need a 14 M KOH (784 g L^{-1}) solution to precipitate.

This work presents the first attempt to adapt and improve the microwave one-step flash synthesis for the production of Fe–Co alloy/cobalt ferrite nanocomposites. Obviously, the products will be compared with those prepared by the conventional route (i.e. conventional heating in boiling KOH).

2. Experimental

2.1. Operating conditions

All the chemicals products, $FeCl_2 \cdot 4H_2O$ (Prolabo, Normapur), $CoCl_2 \cdot 6H_2O$ (Prolabo, Normapur), sodium ethoxide (EtONa, Aldrich, 96%) and ethanol (Prolabo, Normapur, 96%) were reagents grade used without further purification. Concentrations were chosen according to results obtained in a previous study [17]; this gave guidelines to set the initial Co/Fe to a value of 0.5. Consequently, the iron salt concentration is fixed at 0.2 M, the cobalt salt concentration at 0.1 M and sodium ethoxide concentration at 1 M.

Different heating times (from 10 s to 10 min) were tested. The reactants have been treated by microwave induced thermal hydrolysis with the help of an autoclave microwave heating device. Compared to domestic ovens, this experimental set up is constituted by a microwave applicator associated with an autoclave. This was specially designed by the authors and a more detailed description is available in Refs. [17–22]. A fiber optic thermometry system allows measuring precisely the temperature within the reactor.

Solution of sodium ethoxide in ethanol was prepared at room temperature and poured into the autoclave. In order to avoid oxidation, ferrous chloride and cobalt chloride were dissolved in ethanol just before use and poured at rate of 2 mL by minute into the solution of sodium ethoxide. At this stage, a green-black precipitate occurs.

From this point, the reactor was quickly sealed and an argon pressure introduced (0.4 MPa). Here starts the second step of the synthesis where the microwave heating is involved. First of all, a microwave power (1 kW) is applied until the pressure reaches a threshold value of 1 MPa. At this point, the temperature is close to 160°C [17]. A crude estimation of the heating rate gives an average value of 10°C s^{-1}. When the threshold value is obtained, the pressure is maintained according to selected durations (from 10 s to 10 min).

After this thermal treatment, the as-synthesized powders were centrifuged and washed with distilled water in order to eliminate sodium and chloride ions. Finally, they were lyophilizing in order to remove any remaining solvent.

2.2. Characterization methods

The powders were fully characterized using X-ray diffractions techniques as well as via extensive electron microscopy. XRD measurements were performed at room temperature using a D5000 Siemens diffractometer equipped with a monochromatic beam Cu$K\beta$ ($\lambda = 0.139$ nm) focused with a secondary curved graphite monochromator. Patterns were collected in the 25–60° 2θ range with a step increment of 0.03° 2θ. The counting time was fixed to 100 s per step in order to optimize the signal to noise ratio. Microstructural information was extracted from the diffractograms using the profile-fitting program PROFILE. Indeed, the pattern decomposition allows the estimation of pertinent parameters (position, area, height, integral width) for Bragg reflections of spinel phase. An average crystallite size was calculated from the XRD profile analysis using the method described by Langford [23]. In the mean time, the cell parameters were determined by a least-squares refinement program (celref [24]).

High-resolution transmission electron microscopy (HRTEM) fitted with an energy-dispersive X-ray spectroscopy (EDSX) system was used to gather microstructural information about the as-produced powders such as the phase identification, the individual grain compositions or the phase distribution within particles. The samples were prepared using two main techniques:

(1) Depositing the powder dispersed into ethanol on to a holey carbon coated 200 mesh copper grid.
(2) Embedding the powder into an Epon 812 resin, then cut thin slices using an ultramicrotome equipped with a diamond knife. The 60–90 nm thick sections were then collected on a holey, carbon coated, 200 mesh copper grid.

The samples were examined with a TOPCON 002B microscope operating at 200 kV (point to point resolution of 0.18 nm) and equipped with an ultrathin window KEVEX EDX spectrometer.

Metallic iron and cobalt ferrite present magnetic properties. The irreversibility of magnetization mechanisms is traduced by a hysteresis cycle. In this study, the hysteresis cycles of the composite were recorded at room temperature with a Foner type apparatus.

3. Results and discussion

Fig. 1 displays the XRD patterns obtained after different holding time (10 s to 10 min). All the samples show well-defined X-ray diffraction patterns and very low backgrounds indicating a good crystallization despite any heat treatment was carried out on powder. The major phases identified are a spinel phase ($Fe_{3-x}Co_xO_4$) and a metallic phase (Fe_yCo_{1-y}) in agreement to patterns recorded after conventional synthesis [25]. Fe (II) in the Fe $(OEt)_2$ form disproportionates under microwaves in an alcoholic media as it was previously shown in an aqueous media [13,25]. The disproportionation reaction is

$$3Fe(OEt)_2 \rightarrow 2Fe(OEt)_3 + Fe^0. \quad (1)$$

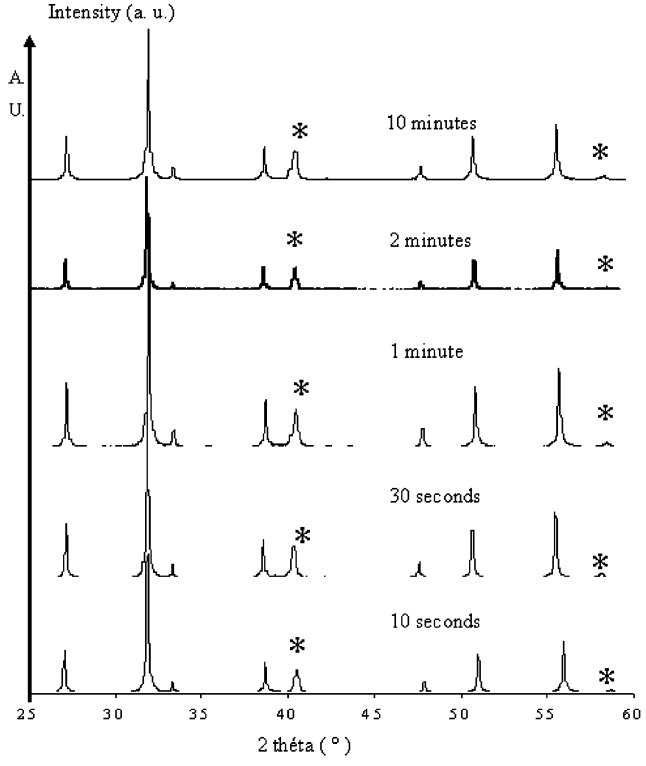

Fig. 1. X-ray diffraction patterns of Fe–Co alloy/Cobalt ferrite synthesized from [EtONa] = 1 M, $[Fe^{2+}] = 0.2$ M, $[Co^{2+}] = 0.1$ M. The * correspond to the Fe–Co alloy diffraction lines. The other diffraction lines correspond to the spinel phase.

A cobalt ferrite $Fe_{3-x}Co_xO_4$ is given by hydrolysis and condensation due to presence of $Co(OEt)_2$, $Fe(OEt)_2$ and $Fe(OEt)_3$ in solution as described by

$$x\,Co(OEt)_2 + 1 - x\ Fe(OEt)_2 + 2Fe(OEt)_3 + 4H_2O \rightarrow Fe_{3-x}Co_xO4 + 8EtOH. \quad (2)$$

Metallic cobalt is formed by partial reduction of Co(II) because Co(II) is able to be reduce by metallic iron:

$$Co^{2+} + 2e^- \leftrightarrow Co^0, \quad E_0 = -0.28\ V, \quad (3)$$

$$Fe^{2+} + 2e^- \leftrightarrow Fe^0, \quad E_0 = -0.44\ V. \quad (4)$$

Metallic iron and metallic cobalt give an intermetallic phase:

$$yFe^0 + 1 - yCo^0 \rightarrow Fe_yCo_{1-y}. \quad (5)$$

Small quantities of akaganeïte (β-FeOOH) or hematite (α-Fe_2O_3) are present whatever the holding time is. When mixing is carried out under inert atmosphere, these parasitic phases are not detected. Also, these impurities are formed by oxidation of ferrous ions by ambient oxygen of air during mixing of the two solutions.

For all the synthesis, the powders are composed of the same two phases (oxide and metal). The product formation occurs inside the microwave reactor very quickly (i.e. less than 10 s) and does not depend on the heating duration. No modification of the cell parameters (spinel $a = (0.8398 \pm 0.0003)$ nm) have been observed even if the microwave heating is hold during 10 min. This last result is in opposition with results obtained previously when only ferrous chloride is involved [17]. The XRD estimated cell parameter is larger than both theoretical cell-parameters of magnetite (0.8396 nm [26]) and cobalt ferrite (0.8392 nm [27]). Nevertheless, this value is in accordance with cell parameters obtained by Pourroy et al. [28] on cobalt–iron alloy/cobalt ferrite powders obtained by coprecipitation of hydroxides in boiling KOH.

The Langford approach enables to extract from the XRD profile analysis data an estimation of mean crystallite size. It has been clearly established that the mean crystallite size for spinel phase is fairly close to 100 nm. In addition, no major modifications have been observed when the heating duration is increased.

The morphology of the as-produced powders has been exhaustively investigated using electron microscopy. Fig. 2 gives examples of the typical TEM bright field images obtained for different heating time. In all the cases, three classes of crystallites are observed whatever the heating duration is:

(1) Elementary spherical grains with a diameter close to 20 nm; the EDSX analysis indicate a large percentage of iron, cobalt and oxygen in those particles. Consequently, these grains correspond to the cobalt

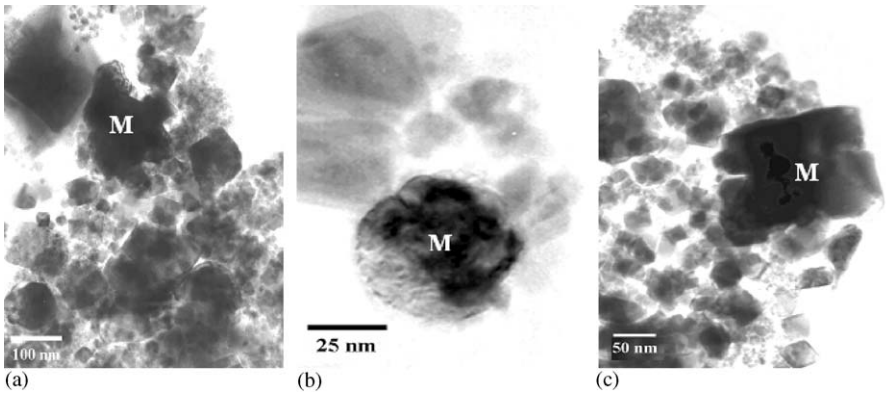

Fig. 2. TEM micrographs of Fe–Co alloy/Cobalt ferrite synthesized from $[Fe^{2+}]=0.2$ M, $[Co^{2+}]=0.1$ M and [EtONa] = 1 M treated 10 s (a), treated 1 min (b) and treated 10 min (c). M correspond to the Fe–Co alloy crystals.

ferrite phase identified in the XRD patterns.

(2) Particles in form of lozenge with a size between 50 and 200 nm; they contain iron, cobalt and oxygen. These particles correspond also to the cobalt ferrite phase.

(3) Grains without particular form with a size between 40 and 200 nm; they contain only iron and cobalt. These particles correspond to the metallic Fe/Co alloy.

EDSX analysis shows that no sodium and chlorine are present in the powders. More important, they unveiled a specific distribution of Fe and Co depending on the phase: metallic areas are cobalt rich and oxide areas are iron rich. As seen before, metallic cobalt is obtained by partial reduction of Co(II) by metallic iron. Also, microwave treatment particularly enhances the oxido-reduction between metallic iron and Co(II).

When no Co is added to the reactant mixture, two types of spinel crystals were detected for heating times superior at 4 min [17]. If a significant amount of Co is added, the dual spinel phase crystal distinction is obtained much quicker. The necessary time is certainly under 10 s. On the assumption that the second type of crystals (2) is formed by dissolution-recrystallization from the first type (1), the kinetic of reaction seems to be more significantly improved when cobalt is added to ferrous ions.

Fig. 3 detailed the surface of cobalt ferrite crystals which appear in form of lozenge (2) for 10 s (a) and 1 min (b) of heating time. Both look like fine platelets without major defects. When Figs. 3(a) and (b) are closely compared, a clear 5 nm thick superficial layer appears to wrap the crystallite surface for the longer microwave treatment. Further studies to investigate this layer and to find the above reaction mechanism are underway.

The main difference between similar composites produced using a conventional heating [29] and a microwave treatment is the microstructure of the end-

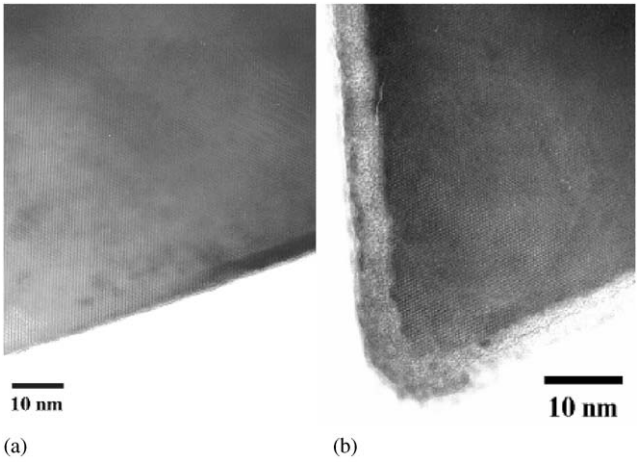

Fig. 3. TEM micrographs of Cobalt ferrite synthesized from $[Fe^{2+}]=0.2$ M, $[Co^{2+}]=0.1$ M and [EtONa] = 1 M treated 10 s (a) and 1 min (b).

product. In the case of a conventional heating, only one type of crystal is obtained and the metallic phase is embedded in oxide phase. For the microwave heating, oxide and metal crystals are separated. In addition, smaller grain size is obtained in microwave synthesis in a less basic medium. The amount of each phase in the composite is difficult to measure directly using any TEM based technique. The thermogravimetric route unfortunately underestimates this percentage because of the presence of adsorbed water. Anyway, a first estimation gives a metallic phase percentage close to 20%. This value is smaller than the amount obtained for conventional heating (close to 50%).

As the composites are made of magnetic phases, these phases can be characterized by magnetic measurements. Fig. 4 presents the hysteresis cycle recorded at 300 K for a sample heat treated 10 min. This measurement gives a saturation magnetization (S) and a coercitivity (H) in the range of 90 emu g^{-1} and 1000 Oe, respectively for all the powders. This value does not fluctuate with the

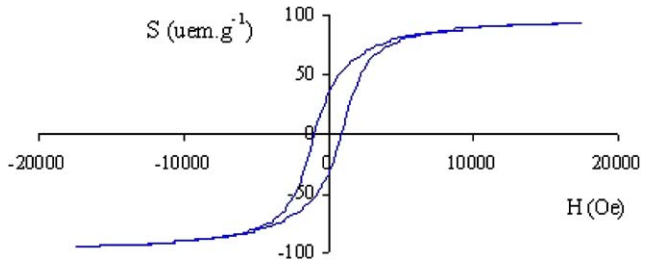

Fig. 4. Hysteresis cycle recorded at 300 K on the sample synthesized from $[Fe^{2+}] = 0.2$ M, $[Co^{2+}] = 0.1$ M and [EtONa] = 1 M treated 10 min.

heating duration. The magnetization is not completely saturated for the maximum Field (18,000 Oe) and values are in accordance with magnetization obtained on samples prepared by conventional heating [30]. On the contrary, coercive field is lower than the 2300 Oe reported for conventional synthesis. The lower grain size obtained during the microwave process (100 nm compared to 0.1–0.5 μm for the conventional heating) and the difference in microstructure can explain this difference.

4. Conclusion

This paper has presented for the first time an original microwave hydrothermal flash synthesis of Fe–Co alloys (Fe_yCo_{1-y})/cobalt ferrite ($Fe_{3-x}Co_xO_4$) nanocomposites. Two different spinel phases are concomitantly produced during very short heating time (i.e. 10 s). Consequently, the kinetic of reaction might be enhanced when cobalt is added at ferrous ions. Oxide and metal are clearly separated phases within the powders. In addition, small grains (100 nm) are obtained in microwave synthesis in a less basic medium. These results distinguish the microwave flash synthesis from the conventional route for which larger grains form a composite where the metallic phase is embedded within the oxide.

The microwave treatment clearly speeds up the synthesis process with energy saving as shown before [31,32]. The time saving factor is close to 10 comparing with similar composites obtained by using conventional heating of aqueous solution. Nevertheless, the amount of metal inside the composite powder is still low (i.e. 20% versus 50% for the conventional heating). Further work is required to improve the output of the technique as well as a better understanding of the process by itself. In the future, it would be interesting to characterize each phases produced during the microwave treatment. The use of a Rietveld analysis program [33] as XND [34] might help to differentiate the two spinel contributions in Bragg reflections in order to get a real image of volumique composition after synthesis. Mössbauer experiments might also provide valuable information.

Acknowledgments

The author which to express their thanks to M.B. Gillot and M.C. Gras for fruitful discussion and encouragement's.

References

[1] S. Komarneni, J. Mater. Chem. 2 (1992) 1219–1230.
[2] F. Tihay, A.C. Roger, A. Kiennemann, S. Läkamp, G. Pourroy, Catal. Today 58 (2000) 263–269.
[3] C. Cabet, A.C. Roger, A. Kiennemann, S. Läkamp, G. Pourroy, J. Catal. 173 (1998) 64–73.
[4] J.C. Yamegni-Noubeyo, G. Pourroy, J. Werckmann, A. Malats i Riera, G. Ehret, P. Poix, J. Am. Ceram. Soc. 79 (1996) 259–270.
[5] G. Pourroy, N. Viart, S. Läkamp, J. Magn. Magn. Mater. 203 (1999) 37–40.
[6] P. Matteazzi, G. Le Caer, J. Am. Ceram. Soc. 75 (1992) 2749–2755.
[7] S.R. Rudge, T.L. Kurtz, C.R. Vessely, L.G. Catterall, D.L. Williamson, Biomaterials 21 (2000) 1411–1420.
[8] S.R. Mekala, J. Ding, J. Alloys Compds. 296 (2000) 152–156.
[9] E. Flahaut, A. Peigney, Ch. Laurent, Ch. Marlière, F. Chastel, A. Rousset, Acta Mater. 48 (2000) 3803–3812.
[10] R. Mathur, D.R. Sharma, S.R. Vadera, S.R. Gupta, B.B. Sharma, N. Kumar, Nanostruct. Mater. 11 (1999) 677–686.
[11] A. Rousset, J. Solid State Chem. 111 (1994) 164–171.
[12] H. Zhang, R. Qi, D.G. Evans, X. Duan, J. Solid State Chem. 177 (2004) 772–780.
[13] S. Läkamp, A. Malats i Riera, G. Pourroy, P. Poix, J.L. Dormann, J.M. Grenèche, Eur. J. Solid State Inorg. Chem. 32 (1995) 159–168.
[14] J.C. Yamegni-Noubeyo, T. Bouakham, G. Pourroy, J. Werckmann, G. Ehret, J. Solid State Chem. 135 (1998) 210–217.
[15] S. Läkamp, G. Pourroy, Eur. J. Solid State Inorg. Chem. 34 (1997) 295–308.
[16] S. Läkamp, G. Pourroy, J. Solid State Chem. 123 (1996) 109–114.
[17] T. Caillot, D. Aymes, D. Stuerga, N. Viart, G. Pourroy, J. Mater. Sci. 37 (2002) 5153–5158.
[18] K. Bellon, D. Chaumont, D. Stuerga, J. Mater. Res. 16 (2001) 2619–2622.
[19] E. Michel, D. Stuerga, D. Chaumont, J. Mater. Sci. Lett. 20 (2001) 1593–1595.
[20] D. Stuerga, M. Delmotte, in: A. Loupy (Ed.), Microwaves in Organic Synthesis, Wiley-VCH Press, Weinheim, Germany, 2003 (Chapter 1).
[21] J.L. Mousson, C. Lohr, P. Pribetich, D. Stuerga, in: C. Folz, J.H. Booske, D.E. Clark, J.F. Gerling (Eds.), Microwave and Radio Frequency Applications "Bridging Science, Technology and Applications", The American Ceramic Society Press, Westerville, OH, USA, 2003, p. 3.
[22] C. Lohr, P. Pribetich, D. Stuerga, Microwave Opt. Technol. Lett. 42 (2004) 46–50.
[23] J.I. Langford, in: Proceedings of the international Conference Accuracy in Powder Diffraction II, NIST, Gaithersburg, MD, May 26–29, 1992.
[24] J. Laugier, B. Bochu, Celref for Windows Unit Cell Refinement Program, ENSP/Laboratoire des Matériaux et du genie physique, France.

[25] G. Pourroy, S. Läkamp, S. Vilminot, J. Alloys Compds. 244 (1996) 90–93.
[26] Powder Diffraction File, International Center for Diffraction Data, File 19-629.
[27] Powder Diffraction File, International Center for Diffraction Data, File 22-1086.
[28] S. Läkamp, G. Pourroy, J. Solid State Chem. 123 (1996) 109–114.
[29] G. Pourroy, A. Valles-Mingues, I.S. Jurca, C. Meny, N. Viart, P. Panissod, J. Alloys Compds. 333 (2002) 296–301.
[30] A. Malats i Riera, G. Pourroy, P. Poix, J. Magn. Magn. Mater. 125 (1993) 125–128.
[31] S. Komarneni, R. Roy, Q.H. Li, Mater. Res. Bull. 27 (1992) 1393–1405.
[32] S. Komarneni, Ionics 21 (1995) 95–98.
[33] H.M. Rietveld, J. Appl. Crystallogr. 2 (1969) 65–71.
[34] J.F. Bérar et, G. Baldinozzi, IUCR-CPD Newsletter 20 (1998) 3–5.